

Electron–phonon interaction and electronic decoherence in molecular conductors

Horacio M. Pastawski^{a,*}, L.E.F. Foa Torres^a, Ernesto Medina^b

^a *Facultad de Matemática Astronomía y Física, Universidad Nacional de Córdoba, Ciudad Universitaria, 5000 Córdoba, Argentina*

^b *Centro de Física, Instituto Venezolano de Investigaciones Científicas, Apartado 21827, Caracas 1020A, Venezuela*

Received 12 October 2001

Abstract

We perform a brief but critical review of the Landauer picture of transport that clarifies how decoherence appears in this approach. On this basis, we present different models that allow the study of the coherent and decoherent effects of the interaction with the environment in the electronic transport. These models are particularly well suited for the analysis of transport in molecular wires. The effects of decoherence are described through the D’Amato–Pastawski model that is explained in detail. We also consider the formation of polarons in some models for the electron–vibrational interaction. Our quantum coherent framework allows us to study many-body interference effects. Particular emphasis is given to the occurrence of anti-resonances as a result of these interferences. By studying the phase fluctuations in these soluble models we are able to identify inelastic and decoherence effects. A brief description of a general formulation for the consideration of time-dependent transport is also presented. © 2002 Elsevier Science B.V. All rights reserved.

PACS: 71.38.–k; 73.40.Gk; 85.35.Be

Keywords: Electron–phonon; Decoherence; Molecular devices; Tunneling time

1. Introduction

Electronic transport in biological and organic molecules has become a very exciting field [1,2] that brings together ideas and results developed during the past two decades in many branches of Physics, Chemistry and Biology. On the basis of this synergic interaction one can foresee very innovative results. Much of its wealth comes from the fact that molecules are intrinsically quantum objects, and quantum mechanics always defies our classical intuition. When this happens, we are almost certain to find new “unexpected phenomena” leading to prospective applications. In turn, with a few exceptions, it is not yet clear how Nature exploits quantum effects in biological systems. However, it seems likely that evolution has made use

* Corresponding author. Fax: +54-351-4334-054.

E-mail address: horacio@famaf.unc.edu.ar (H.M. Pastawski).

of the details of the quantum tunneling process in modulating charge transport [3]. Hence, by pursuing an exploration of dynamical quantum phenomena at the molecular level one may also expect to be more prepared to discover Her hidden ways.

A paradigmatic example of the above situation is the electron transfer in DNA strands [2]. There is evidence that at least two mechanisms are present in this case: (1) A coherent tunneling between the base pairs constituting the donor and acceptor centers. (2) An inelastic sequential hopping through bridging centers. Theoretically, there is a need to unify the description of these extreme regimes as well as to study the possible role of vibrations and distortions of the DNA structure. Our present understanding of these basic physical processes comes from the field of Quantum Transport, which evolved from the description of non-crystalline materials [4] and reached its climax with nanoelectronic [5] devices. Since these last structures may have a very small length scale the term “artificial atoms” [6] is amply justified. Many of the phenomena appearing in these systems could be summarized in the fact that the wave nature of electrons made them susceptible to interference phenomena. These can be assimilated to the propagation of light in some complex Fabry–Perrot interferometer producing either well-defined fringes or “speckle-patterns”. Failures in that simplistic description is essentially due to interactions with excessively complex environmental degrees of freedom (such as thermal vibrations), and our lack of control over them is interpreted as “decoherence” [7]. This often justifies the use of a classical description of the transport process. However, if one is to borrow some idea from the theory of solid state physics, it could be that coherent interactions between electrons and lattice distortions give rise to new effects such as assisted tunneling [8] or even superconductivity. Indeed both phenomena could give striking results in organic systems [9,10]. One is then compelled to develop new tools to describe electron–phonon (e–ph) coherent processes in molecular devices.

In what follows we will make a brief description of quantum interference phenomena establishing a ground level language based on the simplest physical models. While following our personal pathway of many years through the general ideas of transport in the quantum regime, we expect to induce a new perspective into the subtle mechanisms that lead to the degradation of the simple quantum effects through the interactions with the environment (i.e. decoherence). As a token, we will visualize coherent effects emerging from the electron–lattice interaction that can be exploited in new useful ways.

In Section 1 we recall the Landauer ideas [11] for transport which will also serve to adopt a basic language and gives a conceptual framework into which the phenomenological aspects of decoherence can fit. In Section 2 we review the D’Amato–Pastawski (DP) model [12] for coherent and decoherent transport commenting its strengths and limitations. In Section 3 we introduce a polaronic model that hints at the properties of the complete e–ph Fock space. This not only sheds light on the decoherence process but can also be used to predict new phenomena such as the coherent emission of phonons. We devote Section 4 to a brief description of the time dependent transport. Section 5 gives a general perspective.

2. Landauer’s picture for transport

The framework that inspired most of the described experimental developments in mesoscopic electronics was the Landauer’s [11] simple but conceptually new approach. Besides the “sample” or device, he explicitly incorporated the description of the electric reservoirs connected to “the sample”. The role of reservoirs can be played not only by electrodes but also could be spatial regions (localized LCAO) where the electrons lose their quantum coherence. This last situation describes transport in the hopping regime [13] (we will see more on this latter). The simplest mathematical description is obtained if one thinks them as one-dimensional wires that connect the individual orbitals i to electronic reservoirs characterized by the statistical distribution function $f_i(\varepsilon)$. In that case, the electronic states are plane waves describing the different boundary conditions of electrons “in” or “out” the reservoir. An electron out from reservoir connected to “site” i has a probability $T_{j,i}(\varepsilon)$ to enter the reservoir connected to site j . A representation of

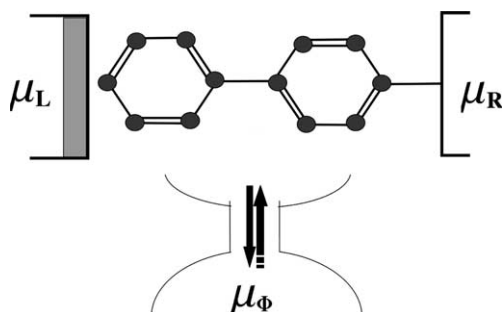


Fig. 1. Representation of a three probe measurement. The voltmeter may be strongly coupled and is a source of decoherence.

such a situation for the case of three reservoirs is sketched in Fig. 1. The current per spin state injected by reservoir j is obtained by the application of the Kirschhoff's law (i.e. a balance equation [13])

$$I_j = e \int d\varepsilon \sum_i \left[T_{i,j}(\varepsilon) v_j \frac{1}{2} N_j f_j(\varepsilon) - T_{j,i}(\varepsilon) v_i \frac{1}{2} N_i f_i(\varepsilon) \right]. \quad (1)$$

The meaning of this equation is obvious: it balances currents. Each reservoir j emits electrons with an energy availability controlled by a Fermi distribution function $f_i(\varepsilon) = 1/[\exp[(\varepsilon - \mu_i)/k_B T] + 1]$, with a chemical potential, $\mu_i = \mu_0 + \delta\mu_i$, displaced from its equilibrium value μ_0 . One can assimilate $V_i = \delta\mu_i/e$ as voltages. The density of those outgoing states is $\frac{1}{2}N_i(\varepsilon)$ (half the total) and their speed v_i . It was essential in Landauer's reasoning to note that in a propagating channel the density of states N_i is inversely proportional to the speed obtained from the corresponding group velocity

$$N_i \equiv 2/(v_i h). \quad (2)$$

This is immediately satisfied in one-dimensional wires but its validity is much more general. This fundamental fact remained unnoticed in the early discussions of quantum tunneling [5] and it is the key to understand conductance quantization. The $G_{j,i} = e^2/h T_{j,i}(\varepsilon)$ are hence Landauer's conductances per spin channel. For perfect transmitting samples $T_{j,i}$ is either 1 or 0 and one obtains the conductance quantization in integer multiples of e^2/h .

Notice that there is no need for the traditional $[1 - f_j(\varepsilon)]$ factor to exclude transitions to already occupied final states. In a scattering formulation, any in state contains a linear combination of out states. Although two different in states (e.g. on the left and right electrodes) could end in the same final out state, unitarity of quantum mechanics assures that both sets are orthogonal. Here the transmission coefficients may depend on the external parameters such as voltages.

An important particularity of our Eq. (1) is that it does not exclude sites $i = j$ from the sum. This contrasts with the original multichannel description [14] and is of utmost importance in the treatment of time dependent problems where $V_i = V_i(t)$ as will be seen in Section 4. Our Eq. (1), always used with Eq. (2), has a full quantum foundation within the Keldysh formulation of Quantum Mechanics (e.g. Ref. [15], Eqs. (5.6–7)). It can be fully expressed in terms of quantities obtained from a Hamiltonian model such as local density of states and Green's functions. We adopt here a notation consistent with these formal developments.

2.1. Phenomenology of decoherence

A first alternative to include decoherence in steady state quantum transport was inspired in the Landauer's formulation. There, the leads, while accepting a quantum description of their spectrum of

propagating excitations, are the ultimate source of irreversibility and decoherence: electrons leaving the electrodes toward the sample are completely incoherent with the electrons coming from the other electrodes. In fact, it is obvious that a wire connected to a voltmeter, by “measuring” the number of electrons in it, must produce some form of “collapse” of the wave function leading to decoherence (see Fig. 1). Besides, no net current flows toward a voltmeter. The leads are then a natural source of decoherence which can be readily described in the Landauer picture if one uses the Landauer conductances together with the Kirchhoff balance equations. This fact was firstly realized by Büttiker [16]. Let us see how it works for the case of a single voltmeter in the linear response regime. In matrix form

$$\begin{pmatrix} I_L \\ I_\phi \\ I_R \end{pmatrix} = \begin{bmatrix} [G_{L,R} + G_{\phi,L}] & -G_{L,\phi} & -G_{L,R} \\ -G_{\phi,L} & [G_{R,\phi} + G_{L,\phi}] & -G_{\phi,R} \\ -G_{L,R} & -G_{R,\phi} & [G_{\phi,R} + G_{L,R}] \end{bmatrix} \begin{bmatrix} V_L \\ V_\phi \\ V_R \end{bmatrix}. \quad (3)$$

Here the unknowns are I_L , I_R and $V_\phi = \delta\mu_\phi/e$. The second equation must be solved with the voltmeter condition $I_\phi \equiv 0$

$$0 = \frac{e}{h} T_{\phi,L}(\delta\mu_\phi - \delta\mu_L) + \frac{e}{h} T_{R,\phi}(\delta\mu_\phi - \delta\mu_R), \quad (4)$$

giving us $\delta\mu_\phi$ to be introduced in the third equation

$$I_R = -\frac{e}{h} T_{R,L}(\delta\mu_L - \delta\mu_R) - \frac{e}{h} T_{R,\phi}(\delta\mu_\phi - \delta\mu_R) = -I_L \quad (5)$$

to obtain the current

$$I_R = \frac{e}{h} \tilde{T}_{R,L}(\delta\mu_L - \delta\mu_R)$$

with

$$\tilde{T}_{R,L} = T_{R,L} + \frac{T_{R,\phi} T_{\phi,L}}{T_{R,\phi} + T_{\phi,L}}. \quad (6)$$

The first term can be identified with the coherent part, while the second is the incoherent or sequential part, i.e. the contribution to the current originated from particles that interact with the voltmeter. This corresponds to an effective conductance of

$$\tilde{G}_{R,L} = G_{R,L} + (G_{R,\phi}^{-1} + G_{\phi,L}^{-1})^{-1}, \quad (7)$$

which can be identified with the electrical circuit of Fig. 2. This classical view clarifies the competition between coherent and incoherent transport. However, this circuit does not imply that in Quantum Mechanics one cannot modify one of the resistances without deeply altering the others. This fact can become very relevant in partially coherent regimes.

So far with the phenomenology. The next important step is to connect these quantities with actual model Hamiltonians. This connection was made explicit by the contribution of D’Amato and Pastawski [12].

3. The DP model for decoherence

3.1. Reducing the Hamiltonian

Let us first review the basic mathematical background that made possible the selection of a simple Hamiltonian that best represents the complex sample–environment system. The objective was to find a simple way to account for the infinite degrees of freedom of a thermal bath and/or electrodes and use the exact solution in the Landauer’s transport equation. First, we recall that one can always eliminate the

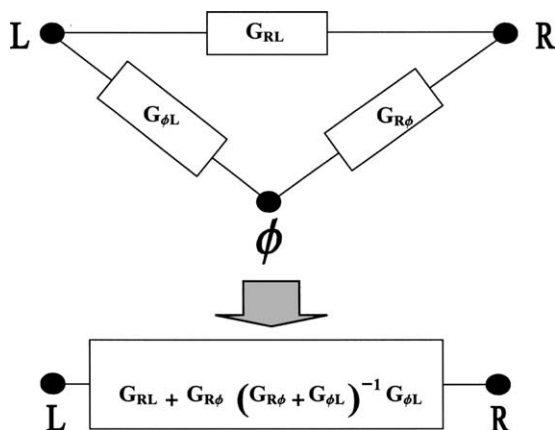


Fig. 2. Classical circuit representation of the non-classical system of Fig. 1.

microscopic degrees of freedom [17,18] generating an effective Hamiltonian, expressed in a basis of localized orbitals. This produces effective interactions and energy renormalizations which depend themselves on the observed energy. Furthermore, one can include a whole lead in a Hamiltonian description through a correction to the eigen-energies which has an *imaginary part*. In fact, an electron originally localized in the region called the sample should eventually escape or decay toward the electrodes. In a microscopic description this is equivalent to the decay of an excited atom according to the Fermi Golden Rule (FGR). Hence, there is a escape velocity associated with the energy uncertainty of a local state

$$v_i = \frac{2a}{\hbar} \Gamma_i = \frac{a}{\tau_i}, \tag{8}$$

where a is a lattice constant. Let us see a simple example. Consider a single LCAO which could be the highest occupied molecular orbital (HOMO) or the lowest unoccupied molecular orbital (LUMO) responsible for resonant transport

$$\widehat{\mathcal{H}}_0^o = E_0 \widehat{c}_0^+ \widehat{c}_0$$

coupled with a *quasi-continuum* of electronic states of the electrode. They are described by a “lead” connected to the voltmeter

$$\widehat{\mathcal{H}}_{\text{lead}} = \sum_k E_k \widehat{c}_k^+ \widehat{c}_k.$$

The sample–lead interaction term is

$$\widehat{\mathcal{H}}_{0\text{-lead}} = \sum_k (V_{k,0} \widehat{c}_k^+ \widehat{c}_0 + \text{c.c.}).$$

The unperturbed atomic energy E_0 will become corrected by the presence of the lead. In second order of perturbation we get

$$\text{lead} \Sigma_0^{R(A)} = \lim_{\eta \rightarrow 0^+} \sum_k \frac{|V_{k,o}|^2}{E_0 - E_k \pm i\eta} = \text{lead} \Delta_0(E_0) \mp i \text{lead} \Gamma_0(E_0). \tag{9}$$

The sign + or – of the infinitesimal imaginary energy η is introduced to handle eventual divergencies in the sum. Since it determines the sign of time in the evolution, the supra-index R or A corresponds to either a retarded or advanced propagation. The imaginary component appears because the electrode spectrum,

described by the density of states $N_{\text{lead}}(\varepsilon)$, is continuum in the neighborhood of energy $E_0 + \Delta(E_0)$. This makes possible the irreversible *decay* into the continuum set of states k , not included in the bounded description. The general functional dependence of $\Delta_0(E_0) - i\Gamma_0(E_0)$ is better expressed in terms of the Wigner–Brillouin perturbation theory

$$\text{lead } \Delta_0(\varepsilon) = \wp \int_{-\infty}^{\infty} \frac{|V_{k,0}|^2}{\varepsilon - E_k} N_{\text{lead}}(E_k) dE_k, \quad (10)$$

where \wp stands for principal value and $N_{\text{lead}}(E_k)$ is the density of states at the lead. Similarly

$$\text{lead } \Gamma_0(\varepsilon) = \pi \int_{-\infty}^{\infty} |V_{k,0}|^2 N_{\text{lead}}(E_k) \delta[\varepsilon - E_k] dE_k. \quad (11)$$

The evaluation of Eqs. (11) and (8) at $\varepsilon = E_0$ constitutes the FGR. Of course these quantities satisfy the Kramers–Kronig relations

$$\Delta_0(\varepsilon) = \frac{1}{\pi} \wp \int_{-\infty}^{\infty} \frac{\Gamma_0(\varepsilon')}{\varepsilon - \varepsilon'} d\varepsilon'. \quad (12)$$

An explicit functional dependence on the variable ε contains eventual non-FGR behavior. The FGR describes reasonably electrons in an atom decaying into the continuum (electrode states), or propagating electrons decaying into different momentum states by collision with impurities or interaction with a field of phonons or photons. In some of these cases, we have to add some degrees of freedom to the sum (the phonon or photon coordinates). A process α may produce contributions ${}^\alpha \Sigma_0^R$ to the total self-energy Σ_0^R

$$\widehat{\mathcal{H}}_0^{\circ} \xrightarrow{\text{interactions}} \widehat{\mathcal{H}}_0 = \widehat{\mathcal{H}}_0^{(\circ)} + \widehat{\Sigma}_0^R(\varepsilon) \quad (13)$$

with

$$\widehat{\Sigma}_0^{R(A)}(\varepsilon) = (\Delta_0(\varepsilon) \mp i\Gamma_0(\varepsilon)) \widehat{\mathcal{C}}_0^+ \widehat{\mathcal{C}}_0 \quad (14)$$

$$= \sum_{\alpha} ({}^\alpha \Delta_0(\varepsilon) \mp i{}^\alpha \Gamma_0(\varepsilon)) \widehat{\mathcal{C}}_0^+ \widehat{\mathcal{C}}_0. \quad (15)$$

Besides, the best way to do perturbation theory to infinite order is the framework of Green's functions.

The unperturbed retarded Green's functions are defined as the matrix elements of the resolvent operator

$$\widehat{\mathbf{G}}^{oR}(\varepsilon) = \lim_{\eta \rightarrow 0^+} [(\varepsilon + i\eta)\widehat{\mathbf{I}} - \widehat{\mathcal{H}}^o]^{-1} \quad (16)$$

for the *isolated* sample. It is practical to represent this as a matrix, $\mathbf{G}^{oR}(\varepsilon)$, whose elements are written in terms of the eigen-energies E_α^o and eigen-functions $\psi_\alpha^{(o)}(\mathbf{r}) = \sum_i u_{\alpha,i} \varphi_i(\mathbf{r})$ of the isolated sample as

$$G_{i,j}^{oR}(\varepsilon) = \lim_{\eta \rightarrow 0^+} \sum_{\alpha} \frac{u_{\alpha,i} u_{\alpha,j}^*}{\varepsilon + i\eta - E_\alpha^o} = [G_{j,i}^{oA}(\varepsilon)]^*. \quad (17)$$

The Local Density of States at orbital i is calculated as

$$N_i^o = \frac{i}{2\pi} \lim_{\eta \rightarrow 0^+} [G_{i,i}^{oA}(\varepsilon) - G_{i,i}^{oR}(\varepsilon)]. \quad (18)$$

The Fourier transform

$$G_{i,j}^{oR}(t_2 - t_1) = \int_{-\infty}^{\infty} \frac{d\varepsilon}{2\pi\hbar} \exp\left[-\frac{i}{\hbar}\varepsilon(t_2 - t_1)\right] G_{i,j}^{oR}(\varepsilon) \quad (19)$$

is solution of

$$\left[\left(-i\hbar \frac{\partial}{\partial t_2} \mathbf{I} + \mathbf{H}^o \right) \mathbf{G}^{oR}(t_2 - t_1) \right]_{ij} = \delta_{ij} \delta(t_2 - t_1) \quad (20)$$

with $t_2 > t_1$. The identity matrix is $\mathbf{I}_{i,j} = \delta_{i,j}$. Hence $G_{i,j}^{oR}(t_2 - t_1)$ is $-i/\hbar$ times the probability amplitude that a particle placed in j th orbital at time t_1 be found in i th one at time t_2 . The advantage of the method is that $G_{i,j}^R(t)$ can be calculated numerically from $G_{i,j}^R(\varepsilon)$ without a detailed knowledge of the eigen-solutions of the perturbed system. For $G_{i,j}^R(\varepsilon)$ one uses:

$$\mathbf{G}^R(\varepsilon) = [\varepsilon \mathbf{I} - (\mathbf{H}_0 + \mathbf{\Sigma}^R(\varepsilon))]^{-1} \quad (21)$$

$$= \mathbf{G}^{oR}(\varepsilon) + \mathbf{G}^{oR}(\varepsilon) \sum_{n=1}^{\infty} [\mathbf{\Sigma}^R(\varepsilon) \mathbf{G}^{oR}(\varepsilon)]^n \quad (22)$$

$$= \mathbf{G}^{oR}(\varepsilon) + \mathbf{G}^{oR}(\varepsilon) \mathbf{\Sigma}^R(\varepsilon) \mathbf{G}^R(\varepsilon). \quad (23)$$

In the second line we have written the usual forms of the Dyson equation from which the Wigner–Brillouin perturbative series and its representation in Feynman diagrams can be obtained. In Fig. 3 we show the graphical representation of the Dyson equation considering two local contributions to the self-energy: the e–ph interactions and the escape to the leads.

For a brief tutorial on the calculation of the Green’s function in discrete systems see [19]. Although the formalism seems to introduce some extra notation it has various conceptual advantages. For example, it is straightforward to use Eq. (21) to prove the *optical theorem* [19]

$$[\mathbf{G}^R - \mathbf{G}^A] = \mathbf{G}^R [\mathbf{\Sigma}^R - \mathbf{\Sigma}^A] \mathbf{G}^A \quad (24)$$

of deep physical significance since it is an integral equation relating the local densities of states given by Eq. (18) and the decay rates provided by Eq. (14) giving Eq. (2). Perhaps the most important advantage, is that they can be used also in the Quantum Field Theory [20,21] to deal with the many-body case.

The direct connection between observables and the transmittances used in the Landauer formulation and the Green’s function follows intuitively from the Green’s function probabilistic interpretation. This was formalized by DP who used a result of Fisher and Lee [22] that related the transmittance to a product of the Green’s function connecting two regions and their group velocities. By noting the discussed relation between the group velocity and the imaginary part of the effective potential established in Eq. (8), DP obtained a simple expression for the transmittance, which in our present notation can be written as

$$T_{j\alpha,i\beta}(\varepsilon) \equiv |t_{j\alpha,i\beta}(\varepsilon)|^2 = [2^\alpha \Gamma_j(\varepsilon)] G_{j,i}^R(\varepsilon) [2^\beta \Gamma_i(\varepsilon)] G_{i,j}^A(\varepsilon). \quad (25)$$

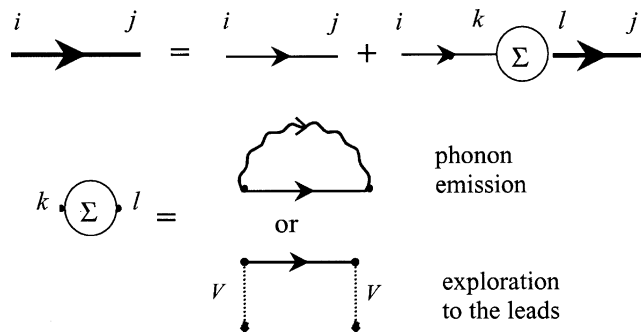


Fig. 3. Feynman representation of the Dyson equation for the single particle Green’s function (line). An e–ph self-energy is evaluated in terms of the sample electron (line) and phonon (wave) Green’s functions. The leads self-energies contain the hopping (dot) and the propagator in the lead.

The left supra-index α in ${}^\alpha\Gamma$ indicates each of the *independent* processes producing the decay from the LCAO modes (right subindex) associated with the physical channel. In the basis of independent channels the complex part of the self-energy is diagonal. Hence the sum over initial states and processes in the physical channels R and L of Eq. (1) determines a conductance including spin channels:

$$\mathbf{G}_{\mathbf{R},\mathbf{L}} = \frac{2e^2}{h} 4\text{Tr}[\Gamma_{\mathbf{R}}(\varepsilon)\mathbf{G}_{\mathbf{R},\mathbf{L}}^{\mathbf{R}}(\varepsilon)\Gamma_{\mathbf{L}}(\varepsilon)\mathbf{G}_{\mathbf{L},\mathbf{R}}^{\mathbf{L}}(\varepsilon)]. \quad (26)$$

This matrix expression is simply a compact way to write Eq. (1), using Eqs. (25) and (8) together to compute the linear response conductance between any pair L and R of electrodes. The sum of initial states at left (L) is the result of the product of the diagonal $\Gamma_{\mathbf{L}}(\varepsilon)$ form of the broadening matrix, while the final trace is the sum over final states at right (R). With different notations, these basic ideas recognize by now many applications to the field of molecular electron transfer [23].

Originally, Fisher and Lee considered only the escape velocity to the leads (i.e. $\alpha = \beta = \text{lead}$). Our point is that *any other process* which contributes to the decay *giving an imaginary* contribution to the *self-energy* would be described by Eq. (25). In particular, this will be true for a “decoherence” velocity that degrades the coherent current. This view was proposed in DP [12] adopting a discrete (tight-binding) description of the spatial variables at each point (or orbital) in the real space a decay rate was assigned which is balanced by the particles reinjection in the same site, described as local reservoirs.

We now show how the DP model applies to a simple tunneling system. Consider the unperturbed Hamiltonian,

$$\widehat{\mathcal{H}}_0 = \sum_{i=1}^N \left\{ E_i \widehat{c}_i^+ \widehat{c}_i + \sum_{j(\neq i)} V_{i,j} [\widehat{c}_i^+ \widehat{c}_j + \widehat{c}_j^+ \widehat{c}_i] \right\}. \quad (27)$$

Since the indices i and j (sites) refer to any set of atomic orbitals, the interactions are not restricted to nearest neighbors. However, for the usual short range interactions, the Hamiltonian matrix has the advantage of being sparse. The local dephasing field is represented by

$$\phi \widehat{\Sigma}^{\mathbf{R}} = \sum_{i=1}^N -i \phi \Gamma \widehat{c}_i^+ \widehat{c}_i, \quad (28)$$

where $\phi \Gamma = \hbar/(2\tau_\phi)$. We consider for simplicity only two one-dimensional current leads L and R connected to the first. and the N th orbital states, respectively,

$$\text{leads } \widehat{\Sigma}^{\mathbf{R}} = -i({}^{\mathbf{L}}\Gamma \widehat{c}_1^+ \widehat{c}_1 + {}^{\mathbf{R}}\Gamma \widehat{c}_N^+ \widehat{c}_N). \quad (29)$$

We see that the first state has escape contributions both, toward the current lead at the left, ${}^{\mathbf{L}}\Gamma_1$, and to the inelastic channel associated to this site, $\phi \Gamma_1$. The on-site chemical potential will ensure that no net current flows through this channel.

3.2. The solution for incoherent transport

To simplify the notation we define the total transmission from the channels at each site as:

$$(1/g_i) = \sum_{j=0}^{N+1} T_{j,i} = \begin{cases} 4\pi N_1^{\mathbf{L}} \Gamma_1 & \text{for } i = 0, \\ 4\pi N_i^{\phi} \Gamma_1 & \text{for } 1 \leq i \leq N, \\ 4\pi N_N^{\mathbf{R}} \Gamma_N & \text{for } i = N + 1. \end{cases} \quad (30)$$

The last equality follows from the optical theorem of Eq. (24). The balance equation becomes

$$I_i \equiv 0 = (1/g_i)\delta\mu_i + \sum_{j=0}^N T_{i,j}\delta\mu_j, \quad (31)$$

where the sum adds all the electrons that emerge from a last collision at other sites (j s) and propagate coherently to site i where they suffer a dephasing collision. These include the electrons coming from the current source i.e. $T_{i,L}\delta\mu_L$ and the current drain. In Eq. (31), since we refer all voltages to the right one, then $T_{i,R}\delta\mu_R \equiv 0$. The first term accounts for all the electrons that emerge from this collision on site i to have a further dephasing collision either in the sample or in the leads. The net current is identically zero at any dephasing channel (lead). The other two equations are

$$I_L \equiv -I = (1/g_1)\delta\mu_L - \sum_{j=0}^N T_{L,j}\delta\mu_j, \quad (32)$$

$$I_R \equiv -I = - \sum_{j=0}^N T_{R,j}\delta\mu_j.$$

Here we need the local chemical potentials which can be obtained from Eq. (31). In a compact notation, these coefficients can be arranged in a matrix form which excludes the leads that are current source and sink:

$$\mathbf{W} = \begin{bmatrix} 1/g_1 - T_{1,1} & -T_{1,2} & -T_{1,3} & \cdots & -T_{1,N} \\ -T_{2,1} & 1/g_2 - T_{2,2} & -T_{2,3} & \cdots & -T_{2,N} \\ -T_{3,1} & -T_{3,2} & 1/g_3 - T_{3,3} & \cdots & -T_{3,N} \\ \vdots & \vdots & \vdots & \ddots & \vdots \\ -T_{N,1} & -T_{N,2} & -T_{N,3} & \cdots & 1/g_N - T_{N,N} \end{bmatrix}. \quad (33)$$

Then, the chemical potential in each site can be calculated from Eq. (31) as

$$\delta\mu_i = \sum_{j=1}^N (\mathbf{W}^{-1})_{i,j} T_{j,0} \delta\mu_0. \quad (34)$$

Replacing these chemical potentials back in Eq. (32) the effective transmission can be calculated

$$\tilde{T}_{R,L} = T_{R,L} + \sum_{j=1}^N \sum_{i=1}^N T_{R,j} [\mathbf{W}^{-1}]_{j,i} T_{i,L}. \quad (35)$$

The first contribution in the RHS comes from electrons that propagate quantum *coherently* through the sample. The second term contains the *incoherent* contributions due to electrons that suffer their first dephasing collision at site i and their *last one* at site j .

Until now the procedure has been completely general, there is no assumption involving the dimensionality or geometry of the sample. The system of Fig. 4 was adopted in DP only because it has a simple

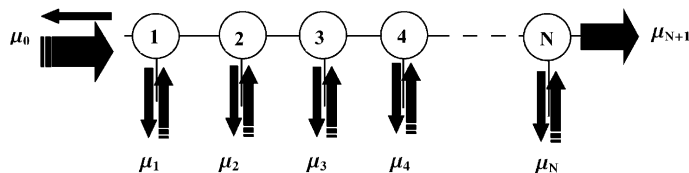


Fig. 4. Pictorial representation of the DP model for the case of a linear chain.

analytical solution for $T_{i,j}$ in various situations ranging from tunneling to ballistic transport. We summarize the procedure for the linear response calculation. First, we calculate the complete Green’s function in a tight-binding model. Since the Hamiltonian is sparse this is relatively inexpensive if one uses the decimation techniques described in [18]. With the Green’s functions, we evaluate the transmittances between every pair of sites in the sample (i.e. nodes in the discrete equation) and write the transmittance matrix \mathbf{W} . Then, we solve for the current conservation equations that involve the inversion of \mathbf{W} .

What are the limitations of this model? A conceptual one is the momentum demolition produced by the localized scattering model. Therefore, by decreasing τ_ϕ , the dynamics is transformed continuously from quantum ballistic to classical diffusive. To describe the transition from quantum ballistic to classical ballistic, one should modify the model to have the scattering defined in phase space or energy basis. While the first is well suited for scattering matrix models [24], the last is quite straightforward as will be shown in next Section. The other aspect is merely computational. Since the resulting matrix \mathbf{W} is no longer sparse, this inversion is done at the full computational cost. A physically appealing alternative to matrix inversion was proposed in DP. The idea was to expand the inverse matrix in series in the dephasing collisions, resulting in

$$\tilde{T}_{R,L} = T_{R,L} + \sum_i T_{R,i} g_i T_{i,L} + \sum_i \sum_j T_{R,i} g_i T_{i,j} g_j T_{j,L} + \sum_i \sum_j \sum_l T_{R,i} g_i T_{i,j} g_j T_{j,l} g_l T_{l,L} + \dots \quad (36)$$

The formal equivalence with the self-energy expansion in terms of locators or local Green’s function justifies identifying g_i as a *locator* for the classical Markovian equation for a density excitation [25] generated by the transition probabilities T s. Notice that Eq. (36) can also be rearranged as

$$\tilde{T}_{R,L} = T_{R,L} + \sum_{i=1}^N \tilde{T}_{R,i} g_i T_{i,L}. \quad (37)$$

This has the structure of the Dyson equation, graphically represented in Fig. 5. We notice that according to the optical theorem $g_i = \tau_\phi 2\pi\hbar N_i$, while both transmittances entering the vertex are proportional to $1/\tau_\phi$, the whole vertex is proportional to the dephasing rate. The arrows make explicit that transmittances are the product of a retarded (electron) and an advanced (hole) Green’s function. Obviously, one can sum the terms of Eq. (36) to obtain the result of Eq. (6) for phenomenological decoherence.

Many of the results contained in the DP paper for ordered and disordered systems were extended in great detail in a series of papers by Datta and collaborators [26] and are presented in a didactic layout in a book. In the following section, we will illustrate how the previous ideas work by considering again our reference toy model for resonant tunneling.

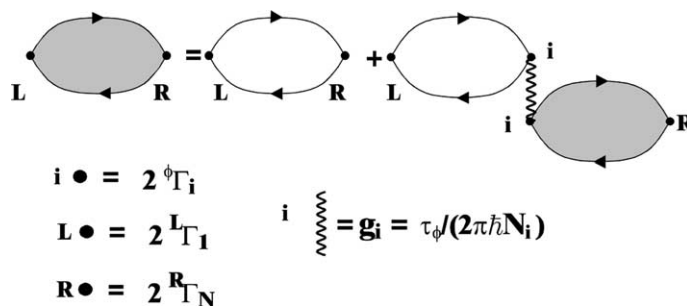


Fig. 5. Feynman diagram for the Dyson equation of the transmittance. It is equivalent to a particle–hole Green’s function in the ladder approximation where a rung is represented by a dot.

3.3. Effects of decoherence in resonant tunneling

After an appropriate decimation [18] the sample is represented by a single state [15]. If we choose to absorb the energy shifts into the site energies $\bar{E}_0 = E_0 + \Delta$, the Green's function is trivial

$$G_{0,0}^R = \frac{1}{\varepsilon - \bar{E}_0 + i(L\Gamma + R\Gamma + \phi\Gamma)}. \quad (38)$$

By taking the Γ s independent on ε in the range of interest we get the “broad-band” limit. From now on we drop unneeded indices and arguments. From this Green's function all the transmission coefficients can be evaluated at the Fermi energy.

$$\begin{aligned} T_{R,L} &= 4^R \Gamma |G_{0,0}|^2 L\Gamma, \\ T_{\phi,L} &= 4^\phi \Gamma |G_{0,0}|^2 L\Gamma, \\ T_{R,\phi} &= 4^R \Gamma |G_{0,0}|^2 \phi\Gamma. \end{aligned} \quad (39)$$

We obtain the energy dependent total transmittance

$$T_{R,L}(\varepsilon) = 4^R \Gamma \frac{1}{(\varepsilon - E_0)^2 + (L\Gamma + R\Gamma + \phi\Gamma)^2} L\Gamma \left\{ 1 + \frac{\phi\Gamma}{L\Gamma + R\Gamma} \right\}. \quad (40)$$

The first term in the curly bracket is the coherent contribution while the second is the incoherent one. We notice that the effect of the decoherence processes is to lower the value of the resonance from its original one in a factor

$$\frac{(L\Gamma + R\Gamma)}{(L\Gamma + R\Gamma + \phi\Gamma)}. \quad (41)$$

In compensation, transmission at the resonance tails becomes increased.

It is interesting to note the results in the non-linear regime when the voltage drop eV is greater than the resonance width $(L\Gamma + R\Gamma + \phi\Gamma)$. If the new resonant level lies between $\mu_0 + eV$ and μ_0 , we can easily compute the *non-linear current* using $T_{R,L}(\varepsilon, eV)$. Notably, one gets that the total current does not change as compared with that in absence of decoherent processes, i.e.:

$$I \frac{\hbar}{2e} = \int_{\mu_0}^{\mu_0 + eV} \tilde{T}_{R,L}(\varepsilon, eV) d\varepsilon = \int_{\mu_0}^{\mu_0 + eV} T_{R,L}^o(\varepsilon, eV) d\varepsilon \quad (42)$$

$$= 4\pi^R \Gamma \frac{1}{(L\Gamma + R\Gamma)} L\Gamma. \quad (43)$$

Thus, in this extreme quantum regime, the *decoherence processes do not affect the overall current*. Such relative “stability” against decoherence is fundamental in the Integer Quantum Hall Effect [27] and should also be present for tunneling through molecular states as both of them have a discrete spectrum. Notice that in this last case the dependence of the escape rates on eV is generally weak. Hence, the experimental value of the current allows an estimation of the escape rate.

We learn important lessons from the case of resonant tunneling with the inclusion of external degrees of freedom as decoherence:

- (1) The integrated intensity of the elastic (coherent) peak is decreased.
- (2) An inelastic current comes out to compensate this loss and maintains the value of the total transmittance integrated over energy.
- (3) Decoherence *broadens* both contributions to the resonance, relaxing energy conservation.

The representation of the e–ph through complex self energies damps the quantum interferences associated with repeated interactions with some vibrational modes that would originate the polaronic states. In

what follows we will explore some simple Hamiltonian models where decoherence is not introduced at such an early stage. Instead of calculating transition rates, the approach will be to consider the many-body problem and to compute the quantum amplitudes for each state in the Fock space.

4. The electron–phonon models

4.1. A state conserving interaction model

Let us consider a simple model that complements that of DP by providing an explicit description of a single extended vibrational mode whose quanta in a solid would be optical phonons,

$$\widehat{\mathcal{H}}_{\text{ph}} = \hbar\omega_0 \widehat{\mathbf{b}}^+ \widehat{\mathbf{b}}. \quad (44)$$

The electrons are described by

$$\widehat{\mathcal{H}}_{\text{e}} = \sum_{i=-\infty}^{\infty} E_i \widehat{c}_i^+ \widehat{c}_i - \sum_{j(i \neq j)} \left[V_{ij} \widehat{c}_i^+ \widehat{c}_j + V_{ji} \widehat{c}_j^+ \widehat{c}_i \right]. \quad (45)$$

The orbitals between 1 and $N = L_x/a$ define our region of interest. Orbitals at the edge are connected with the electrodes, where $V_{ij} = V$, through tunneling matrix elements $V_{0,1} = V_{1,0} \equiv V_L$ and $V_{N,N+1} = V_{N+1,N} \equiv V_R$. The results will be simpler when $V_{L(R)} \ll V$. Electrons and phonons are assumed to be coupled through a local interaction

$$\widehat{\mathcal{H}}_{\text{e-ph}} = \sum_{i=1}^N -V_g \widehat{c}_i^+ \widehat{c}_i (\widehat{\mathbf{b}}^+ + \widehat{\mathbf{b}}). \quad (46)$$

To build the e–ph Fock space we consider a single electron propagating in the leads while the number n of vibronic excitations is well defined. While this election neglects the phonon mediated electron–electron interaction, it still has non-trivial elements that are the basis for the development of the concept of phonon laser (SASER) [28]. This model will be called State Conserving Interaction (SCI).

The *total energy*, which is conserved during the transport process, is

$$E = \varepsilon_k + n\hbar\omega_0 \quad \text{with } 0 \leq \varepsilon_k \leq \varepsilon_F.$$

Here ε_k is the kinetic energy of the incoming electron on the left lead and n is the number of phonons before the scattering process. A scheme of the complete e–ph Fock space is shown in Fig. 6. It is clear that an electron that impinges from the left when the well has n phonons, can escape through the left or right electrodes leaving behind a different number of phonons. Since these are physically different situations, the outgoing channels with different number of phonons are orthogonal and therefore cannot interfere. This is represented in the fact that the sum of transmittances over final channels satisfy unitarity.

The physical analysis of the excitations can be simplified resorting to a new basis to refer the e–ph states. We notice that, if we neglect the interaction with the leads, we can diagonalize the electronic Hamiltonian without affecting the form of the e–ph interaction. First we diagonalize the electronic system finding the annihilation operators $\widehat{c}_\alpha = \sum_{i=1}^N u_{\alpha,i} \widehat{c}_i$ at eigenstates ψ_α with energies E_α and wave functions $u_{\alpha,i} = \langle i | \alpha \rangle$

$$\widehat{\mathcal{H}}_0 = \sum_{\alpha=1}^N E_\alpha \widehat{c}_\alpha^+ \widehat{c}_\alpha \quad \text{and} \quad \widehat{\mathcal{H}}_{\text{e-ph}} = \sum_{i=0}^N -V_g \widehat{c}_\alpha^+ \widehat{c}_\alpha (\widehat{\mathbf{b}}^+ + \widehat{\mathbf{b}}). \quad (47)$$

The Hamiltonian $\widehat{\mathcal{H}}_{\text{e-ph}}$ is just a linear field for the harmonic oscillator where the field amplitude is proportional to the density of the electrons that disturbs the lattice. Hence, the excitations, called Holstein polarons, are easily obtained. The interesting point is that with the proposed Hamiltonian one can diag-

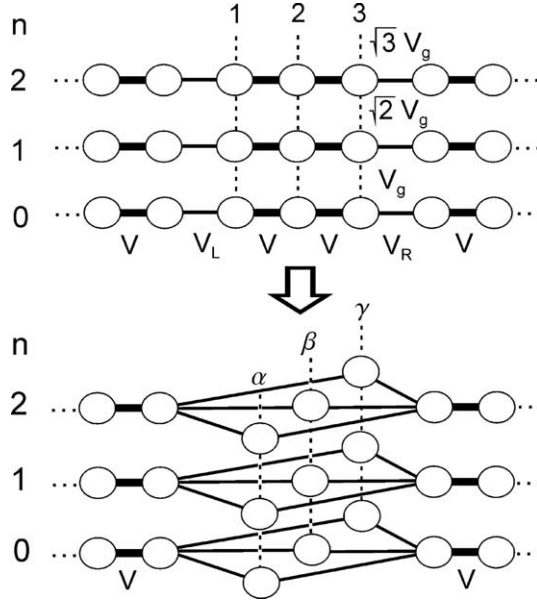


Fig. 6. Scheme for the problem of an electron plus a single phonon mode. The interacting system in the upper figure is transformed into polaronic modes associated to spatial eigenstates which interact weakly through the leads (lower figure).

analyze simultaneously every electron subspace. i.e. in this model the phonons do not cause transitions between electronic levels. The new excitations are described by

$$(\hat{a}_k^+)^n |0_{p,k}\rangle = \sum_{n'=0}^{\infty} \chi_{n,n'} (\hat{b}^+)^{n'} \hat{c}_k^+ |0\rangle, \tag{48}$$

which is valid at every electron space index α . These operators represent polarons in the energy basis analogous to the Holstein’s local polaron model [28,29]. The “polaronic” ground state is related to the vacuum state by $|0_{p,k}\rangle = \sum_{n=0}^{\infty} \chi_{0,n} (\hat{b}^+)^n \hat{c}_k^+ |0\rangle$. The polaronic energies are lower than those of electrons plus phonons

$$E_{\alpha,n'} = E_{\alpha} + \hbar\omega_0 \left(n' + \frac{1}{2} \right) - \frac{|V_g|^2}{\hbar\omega_0} \quad \text{with } n' = \langle \hat{a}^+ \hat{a} \rangle. \tag{49}$$

Since phonons do not produce transitions between electron energy states, this model introduces decoherence through a SCI. The lesson we learn from this is that by writing the interactions in different basis we can choose the quantum numbers that are conserved: e.g. local densities in the DP model and energy eigenstates in the SCI model.

4.2. Coherent and decoherent effects in electronic transport

The general problem of the electronic transport has been solved within the formalism of Keldysh [15,31] in a FGR decoherent approximation [32]. However, here we will solve the full many-body problem. Fig. 6 makes evident that the phonon emission/absorption can be viewed as a “vertical” hopping in a two dimensional network. Once we notice that the Fock-space is equivalent to the electron tight-binding model with an expanded dimensionality [28,30], we see that the transmittances can be calculated exactly from the Schrödinger equation. While excitations are best discussed in the polaronic basis, for the electron transport

it is preferable the use of the asymptotic states. There, when the charge is outside the interacting region, the e–ph product states constitute the natural basis. Recently, this model has gained additional interest as it has been used to explain inelastic effects in STM through molecules [34], to study the transport in molecular wires [35] and to investigate Peierls’s like distortions induced by current in organic compounds [36].

A transport calculation is simpler if we prune the Fock space to include only states within some range of n allowing a non-perturbative calculation which can be considered variational in n . Thus, we are not restricted to a weak e–ph coupling. To obtain the transmittances between different channels several methods can be adopted. One possibility is to solve for the wave function iteratively [33]. An alternative is to obtain Green’s functions to get the transmittances. In this case, the horizontal “dangling chains” in the Fock space can be eliminated through a decimation procedure [12,18] introducing complex self-energies in the corresponding “sites”.

For simplicity, let us consider the case of a single state of energy E_0 in the region of interest which we will call the “resonant” state. It could be interpreted as a HOMO or LUMO state depending on the situation. It interacts with a dispersionless phonon mode, and it is coupled to a source and drain of charge. The problem for an electron that tunnels through the system can be mapped to the one-body problem shown in Fig. 7.

Let us consider an asymptotic incoming scattering state consisting of a wave packet built with e–ph states in the left branch corresponding to n_0 phonons, i.e. an electron coming from the left while there are n_0 phonons in the well. When it arrives at the resonant site where it couples to the phonon field, it can either keep the available energy E as kinetic energy or change it by emitting or absorbing n phonons. Each of these processes contributes to the total transmittance which is given by

$$T_{\text{tot}} = \sum_n T_{n_0+n, n_0}. \quad (50)$$

In Fig. 8(a) we show the total transmittance (thick line) for a case where n_0 is zero and the e–ph coupling is weak. There, the appearance of satellite peaks at energies $E_0 + n\hbar\omega_0$ can be appreciated. To discriminate the processes contributing to the current, we include with a dashed line, the *elastic* contribution to the transmittance, i.e. that due to electrons which are escaping to the right without leaving vibrational excitations behind. This makes almost all of the main peak and only decreasing portions of the satellite peaks. The elastic contribution at the satellite peaks corresponds to a sum of *virtual processes* consisting of the emission of phonons followed by their immediate reabsorption. The *inelastic* component associated with the emission of one phonon is shown with a dotted line.

While the total transmittance (thick line) shows a smooth behavior, the elastic component (dashed line) exhibits a strong dip in the region between the first two resonances. Therefore, almost all of the transmitted electrons within this energy range will be scattered to the inelastic channels. This sharp drop in the elastic transmittance is produced by a destructive interference between the different possible “paths” in the Fock-space connecting the initial and the final channels. These paths can be classified essentially as a direct

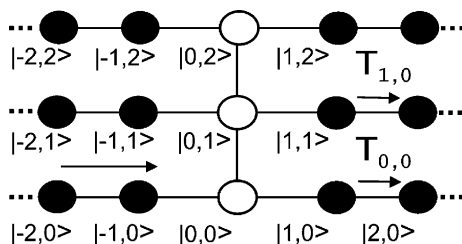


Fig. 7. Each site is a state in the Fock space: The lower row represents electronic states in different sites with no phonons in the well, the sites in black are in the leads. Higher rows correspond to higher number of phonons. Horizontal lines are hoppings and vertical lines are e–ph couplings.

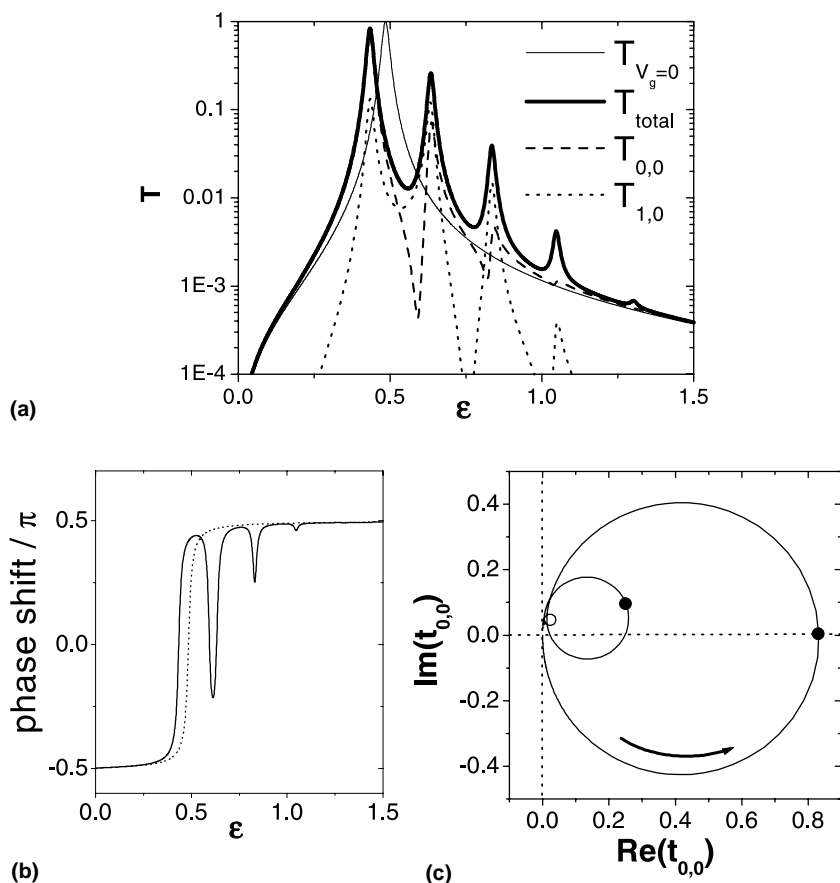


Fig. 8. (a) Transmittance as a function of the incident electronic kinetic energy. The total transmittance is shown with a thick solid line, the elastic component with a dashed line and $T_{1,0}$ with a dotted line. The non-interacting transmittance is also shown with a thin line. In (b) the phase shift of the elastic transmittance as a function of the energy and for the non-interacting case (dotted line) are shown. (c) shows the path of the elastic transmission amplitude in the complex plane when the electronic energy is changed. The full circles correspond to the first and second peaks shown in (a). These results are obtained with $E_0 = -1.5$, $V_L = V_R = 0.1$, $V_g = 0.1$ and $\hbar\omega_0 = 0.2$.

“path” between the incoming and outgoing channels and the same path dressed with virtual emission and absorption processes. The first inelastic component (dotted line) also shows a similar behavior in the valley between the second and third resonances. The main factors that control the magnitude of these *antiresonances* are the escapes to the leads and the e–ph coupling. This concept was introduced in [18,37] to extend the Fano-resonances [38] observed in spectroscopy to the problem of conductance. Perfect antiresonances correspond to situations where both the real and the imaginary part of the transmission amplitude are zero. In the present case, such a perfect interference condition does not occur, and there is a non-zero minimum transmission at the dips. Through a similar analysis one could tailor the geometrical parameters of the system (as done in [39]) to optimize the phonon emission.

An alternative way to appreciate this interference effect is to plot the path followed by the transmission amplitude in the complex plane when the kinetic energy of the incoming electron is changed [40,41]. A plot for the elastic transmission amplitude is shown in Fig. 8(c). For $\epsilon = 0$, there is no transmission. If the energy is increased, one starts to follow the path in the figure anti-clockwise. After reaching the point

corresponding to the first resonance, the transmission starts to decrease and the curve develops a turning near the origin. The first antiresonance takes place at the point of minimum distance from the origin.

In order to rationalize the main processes involved in the first two peaks, let us represent them schematically in Fig. 9. Panel (a) shows the standard elastic process in which no phonon is emitted. Panel (b) is a notable effect that occurs when the phonon emission is virtual. Notice that this virtual process can have strong consequences. In Fig. 8 it produces an increase of the transmittance in almost *two orders of magnitude*. Panel (d) shows a real inelastic process which is expected to give a peak if the initial energy satisfies $E = E_0 + \hbar\omega_0$. Notably, one must expect also a contribution when $\varepsilon = E_0$ which corresponds to the virtual tunneling into the resonant state before emitting a phonon as shown in panel (c).

Another interesting quantity that we can explore with the present formalism is the phase of the transmitted electron through different channels,

$$\eta_{m,n} = \frac{1}{2i} \ln \frac{G_{m,n}^R}{G_{n,m}^A}, \quad (51)$$

whose energy derivative gives information on the dynamics of the process. Fig. 8(b) shows the phase shift of the elastic transmission probability. For reference, the phase shift in the absence of e–ph interaction is also shown with a dotted line. It increases by π over the width of the non-interacting transmission resonance. The same occurs in the interacting case. However, it can be seen that each satellite peak has associated a phase fluctuation. Instead of an increase in the phase by π which would occur for real resonant peaks, across each “satellite peak” associated with the virtual processes, there is a phase dip that results in consecutive resonances having phases close to $-\pi/2$. These phase dips are a manifestation of the anti-resonances shown in Fig. 8(a) for the elastic transmittance. For perfect zero transmission points, one has an abrupt phase fall of π instead of the smooth phase slip shown in the Fig. 8(b) [40].

Let us consider a more general case in which there are initially n_0 phonons in the scattering region. The vertical hopping matrix element connecting states with n_0 and $n_0 + 1$ phonons is $\sqrt{n_0 + 1}V_g$. Then, under these conditions, the adimensional parameter,

$$\tilde{g} = \left(\frac{(\sqrt{n_0 + 1})V_g}{\hbar\omega_0} \right)^2 = (n_0 + 1)g, \quad (52)$$

characterizes the strength of the e–ph interaction. It presents two regimes according to the importance of this interaction.

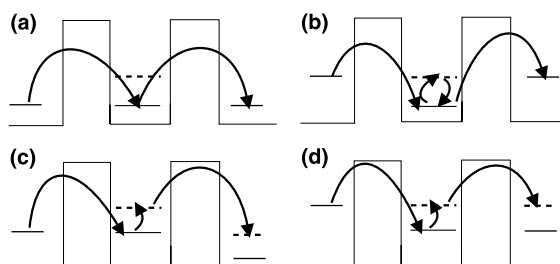


Fig. 9. Schematic representation of the processes that lead to the elastic and inelastic components of the peaks in the total transmittance. (a) and (b) correspond to the first and second peaks of the elastic transmittance, respectively. (c) and (d) correspond to the inelastic part. The well’s ground state is represented by a solid line and the first excited polaron state by a dotted line. The final polaron states at the right of the well are also shown. These states have an energy equal to the incident electron kinetic energy. The final polaron state is depicted with a solid line for the elastic case and with a dotted line for the inelastic situation. The level corresponding to the electron final energy is also shown as a solid line for this case.

In the limit $\tilde{g} \ll 1$ the vertical processes are in a perturbative regime. The “vertical hopping” $\sqrt{n_0 + 1}V_g$ will not be able to delocalize the initial state along this “vertical direction” and therefore the elastic contribution is the most important. In Fig. 10(a), we show with a thick line the transmission probability for a case where $g = 0.25$ in presence of 10 phonons. Notice that “satellite” resonances corresponding to phonon emission and absorption are separated by $\hbar\omega_0$ from the main resonance. For comparison, the curve in absence of e–ph interaction is also included with a dotted line. We see that, as with the DP model, the main resonance peak decreases and presents a general broadening where we can recognize details of the excitation structure of the phonon field. The phase shift as a function of the electronic energy is shown in (b). The solid line is the phase shift for the elastic component of the total transmittance. There, we can appreciate the phase fluctuations that appear even in the elastic transmission.

On the other hand, if $\tilde{g} \gtrsim 1$, the e–ph interaction is in the non-perturbative regime. This can be achieved either by a strong V_g , or by a high n . The second situation would correspond to the case of high temperatures or a far from equilibrium phonon population. In that case, the total transmittance can be obtained by summing the transmittances for the different possible initial conditions weighted by the appropriate thermal factor [42]. In any of these situations, the resulting strong e–ph coupling leads to a breakdown of perturbation theory. A similar case is found for the quantum dots studied in [43]. There, in contrast to the situation in bulk material, the studied quantum dots show a strong e–ph coupling. In molecular wires, where elementary excitations (e or ph) are highly confined, one can expect a similar scenario.

In Fig. 11(a), we show the transmittance as a function of the incident electron kinetic energy for the case where V_g is strong ($\tilde{g} = 4$) and there are no phonons in the well before the scattering process. In contrast to the perturbative regime, where the energy shift of the peaks ($-V_g^2/\hbar\omega_0 = -g\hbar\omega_0$) is small, here the energy shift is important and the inelastic contributions to the total transmittance dominate. In the limit of weak coupling between the scattering region and the leads, the transmission probability through the channel with n phonons becomes the standard Frank–Condon factor: $\exp(-g)^n/n!$.

Fig. 11(b) shows the total transmittance as a function of the incident electron kinetic energy for an extreme case where there are 300 phonons in the well before the scattering process. The electron can absorb or emit as many phonons, $N_{\text{eff}} = 4\sqrt{n}V_g/\hbar\omega_0$, as allowed by the interaction strength. This means that the phonon spectrum, weighted on the local e–ph state n , will be quite independent on the details of the spectral

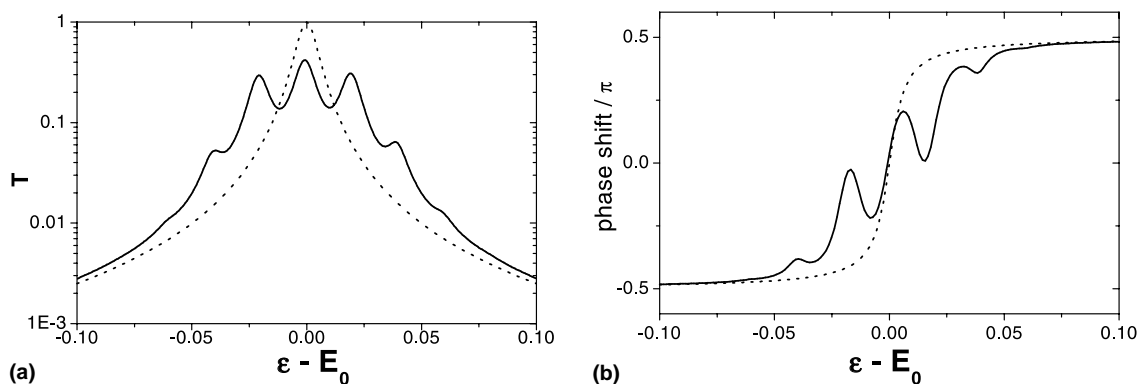


Fig. 10. (a) Total transmittance as a function of the incident electronic kinetic energy. The solid line corresponds to the case in which there are 10 phonons in the well before the scattering process. The dotted line corresponds to the case in which there is no interaction with the vibrational degrees of freedom. (b) Phase shift in units of π as a function of the incident electronic kinetic energy. The solid line is the phase shift for the elastic transmission. The dotted line corresponds to the non-interacting case. The parameters of the Hamiltonian in units of the hopping V are: $E_0 = 0$, $V_L = V_R = 0.05$, $V_g = 0.004$ and $\hbar\omega_0 = 0.02$.

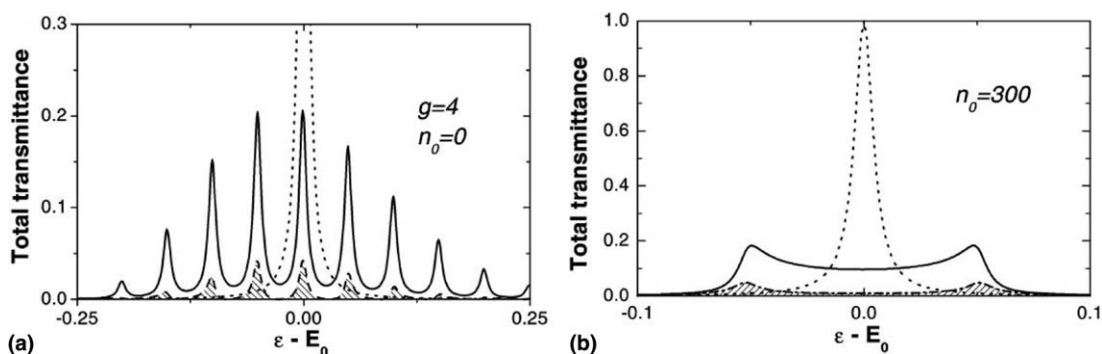


Fig. 11. (a) and (b) show the total transmittance as a function of the incident kinetic electronic energy. The area under the elastic transmittance is filled with a pattern of lines. As before, the dotted line corresponds to the non-interacting case. In (a), the solid line corresponds to the case in which there are no phonons in the well before the scattering process and $V_g = 0.100$, $\hbar\omega_0 = 0.05$. In (b), the solid line corresponds to the case in which there are 300 phonons in the well before the scattering process and $V_g = 0.0015$ and $\hbar\omega_0 = 5.010^{-4}$. The parameters in units of the hopping V are: $E_0 = 0$, $V_L = V_R = 0.05$.

densities at the far end of the effective vertical chain i.e. the states $n \pm N_{\text{eff}}$. Hence, the spectral density will show the typical form of a one dimensional band even when we take $N_{\text{eff}} = 4(V_g/\hbar\omega_0)\sqrt{n} \ll N$. This feature manifests in the transmittance presented in Fig. 11(b). The unperturbed resonant peak is a dotted line which contrasts with the total transmission in presence of phonons shown with a continuous line. Its trace follows the structure of the phonon excitation with the typical square root divergences at the band edges smoothed out by the inhomogeneity in the hopping elements and the uncertainty introduced by the escape to the leads.

5. The solution of time dependence

Finally, we would like to present the basic features of time dependent transport. This is relevant since a coherent “time of flight” should be shorter than any conformational correlation time [44]. The basic idea to get the physics of time dependent phenomena is to obtain the evolution of an arbitrary initial boundary condition of the form $[\psi(X_j)\psi^*(X_k)]_{\text{source}}$. Since here $X_j = (\mathbf{r}_j, t_j)$ with general t_j , this essentially generalizes a density matrix introducing temporal correlations that define the energy of this injected particle. The “density” at a later time is obtained from the exact solution of the Schrödinger equation

$$[\psi(X_2)\psi^*(X_1)] = \hbar^2 \int \int G^R(X_2, X_j) [\psi(X_j)\psi^*(X_k)]_{\text{source}} G^A(X_k, X_1) dX_j dX_k. \quad (53)$$

In order to establish a correspondence with the Danielewicz solution to the Schrödinger equation in the Keldysh formalism, we used the continuous variable Green’s function which is related to the exact discrete one in the *open* system by

$$G^R(\mathbf{r}_i, \mathbf{r}_j, \varepsilon) = \sum_{k,l} G_{k,l}^R(\varepsilon) \varphi_k(\mathbf{r}_i) \varphi_l^*(\mathbf{r}_j). \quad (54)$$

Now, the key is to recognize that in any Green’s function, a macroscopically observable time is $t = \frac{1}{2}[t_j + t_k]$ (time center). Its Fourier transform is an observable frequency ω . Meanwhile, energies are associated with internal time differences $t_j - t_k$ (time chords). Within this scheme, the time correlated initial condition (source), determining the occupation of a local orbital is expressed in terms of the time independent local density of states $N_i(\varepsilon)$

$$[u_i(t)u_i^*(t)]_{\text{source}} = \int \frac{d\varepsilon}{2\pi\hbar} \int d\delta t [u_i(t + \frac{1}{2}\delta t)u_i^*(t - \frac{1}{2}\delta t)]_{\text{source}} \exp[\frac{i}{\hbar}\varepsilon\delta t] = \int d\varepsilon N_i(\varepsilon)f(\varepsilon, t), \quad (55)$$

and the occupation factor $f(\varepsilon, t)$. Introducing this notation in Eq. (53) one can identify the dynamical transmittances $T_{i,j}(\varepsilon, \omega)$. We refer to [15] for a detailed manipulation of the time integrals. The basic result is

$$T_{i,j}(\varepsilon, \omega) = 2\Gamma_i(\varepsilon)G_{i,j}^R(\varepsilon + \frac{1}{2}\hbar\omega)2\Gamma_j(\varepsilon)G_{j,i}^A(\varepsilon - \frac{1}{2}\hbar\omega). \quad (56)$$

The time dependent transmittance is then

$$T_{i,j}(\varepsilon, t) = \int T_{i,j}(\varepsilon, \omega) \exp[-i\omega t] \frac{d\omega}{2\pi}, \quad (57)$$

where one recovers our old steady state transmittance as

$$T_{i,j}(\varepsilon) \equiv T_{i,j}(\varepsilon, \omega = 0) = \int_{-\infty}^t T_{i,j}(\varepsilon, t - t_i) dt_i = \int_t^{\infty} T_{i,j}(\varepsilon, t_f - t) dt_f. \quad (58)$$

Eq. (53) then becomes

$$I_j(t) = \frac{2e}{h} \int d\varepsilon \sum_i \left[T_{i,j}(\varepsilon) f_j(\varepsilon, t) - \int_{-\infty}^t dt_i T_{j,i}(\varepsilon, t - t_i) f_i(\varepsilon, t_i) \right], \quad (59)$$

which is the Generalized Landauer–Büttiker Equation (GLBE) [25,15]. According to Eq. (58), the first term accounts for the particles that are leaving the reservoir at site j at time t to suffer a dephasing collision at some future time at orbital i . The second accounts for particles that having had a previous dephasing collision at time t_i at the i orbital reach site j at time t .

In the GLBE formulation the essential features of time dependence in transport is contained in the transmittances. Since the spectrum is continuous, we can keep the lowest order in the frequency expansion e.g.,

$$T_{i,j}(\varepsilon, \omega) \simeq \frac{T_{i,j}(\varepsilon)}{1 - i\omega\tau_1 + (\omega\tau_2)^2 + \dots}. \quad (60)$$

According to Ref. [15, Eq. (4.5)] the propagation time τ_P is identified with the first significant coefficient in this expansion. Typically, it results the first order,

$$\tau_P = \frac{i\hbar}{2} \left[G_{i,j}^R(\varepsilon) \frac{\partial}{\partial \varepsilon} G_{i,j}^R(\varepsilon)^{-1} + G_{j,i}^A(\varepsilon) \frac{\partial}{\partial \varepsilon} G_{j,i}^A(\varepsilon)^{-1} \right] = -\frac{i\hbar}{2} \frac{\partial}{\partial \varepsilon} \ln \left[\frac{G_{i,j}^R(\varepsilon)}{G_{j,i}^A(\varepsilon)} \right], \quad (61)$$

which can be identified with the Wigner time delay. This propagation time was evaluated in various simple systems in [15] recovering the ballistic and diffusive times for clean and impure metals, respectively. In a double barrier system, in the *resonant tunneling* regime, the propagation time is determined by the life-time inside the well. In fact, using the functions of Section 3.3, one gets for the propagation through the resonant state

$$\tau_P = \frac{\hbar}{2(L\Gamma + R\Gamma)}. \quad (62)$$

From these considerations, we see that τ_P represents a limit to the response in frequency (admittance) of the device. Typically, one gets $G_\omega = G_0/(1 - i\omega\tau_P)$. This is in fair agreement with the experimental results [45].

As another striking example, we mention the “simple” case of *tunneling through a barrier* [46] of length L and height U exceeding the kinetic energy ε of the particle. For barriers long enough the expansion is dominated by the second-order term in Eq. (60) and one gets

$$\tau_P = L / \sqrt{\frac{2}{m}(U - \varepsilon)}, \quad (63)$$

which, within our non-relativistic description, can be extremely short provided that the barrier is high enough. This is the time that one has to compare with vibronic and configurational frequencies [47].

The general propagation times can also be calculated in more complex situations such as disordered systems [48] and those affected by incoherent interactions [15].

6. Perspectives

We have presented the general features of quantum transport in mesoscopic systems. There, interactions with environmental degrees of freedom introduce complex phenomena whose overall effect is to decrease the clean interferences expected for an isolated sample. Such degradation can be accounted for as decoherence. We introduced various simple models which present decoherence. We started presenting the simplest phenomenological models of Büttiker, by discussing its connection with the Hamiltonian description of the DP model. Various simple models for resonant tunneling devices including e–ph interactions were introduced. We feel that they contain the essential coherent and decoherent effects induced by the vibronic degrees of freedom.

Ref. [12] showed that in disordered systems, the effective transmittance away from the resonances keeps its form as a superposition of tails from different resonances. This applies to both the DP and SCI models. This justifies the simplification of using a single resonant state.

Our results for this model make quite clear how complex many body interactions result in the loss of the simple interferences of one body description. Essentially, each external degree of freedom coupled with the electronic states leads to two situations producing decoherence:

- (1) By *real* emission or absorption of phonons, they open additional scattering channels contributing incoherently to the transport. This situation is represented in the DP decoherence model, as well as in the various polaronic models presented here. Those are real processes which can be detected by measuring a change in the bath state (phonon models) or energy dissipated (DP model) within the sample.
- (2) However, even when the e–ph processes might be *virtual*, they would add new alternatives to the quantum phase of the outgoing state. This strongly limits an attempt to control the electron phase and hence is manifested as decoherence.

The study of the coherent component in the presence of decoherent processes gives a first, though imperfect, hint to the conditions of the transport processes. In particular, it can show how decoherence can affect the interference between different propagation pathways. Once they are summed up, the conductance, which is a square modulus, would manifest the effect of a diminished interference. This approach was adopted in a recent work [49] that addressed the delocalizing effect of decoherence on transport in the variable range hopping regime.

It is also worthwhile to mention that the randomization of the quantum phase introduced by the virtual processes can be as much effective [50] as those involving a real energy exchange in producing decoherence. In fact, it has been found recently that this practical uncertainty is the mechanism through which quantum chaos contributes to dissipation and irreversibility [51]. Such quantum chaotic systems have intrinsic decoherence time scales which contrast with the extreme quantum regime of a resonant tunneling where decoherence, if any, is controlled by the environment.

We want to close this section mentioning the connections of the results in Section 4 with other ongoing research on various hot issues of electronic transport. While the problem of tunneling times [46,52] is a controversial one, it has important practical aspects [45]. Indeed, molecular electronics opens the whole issue of quantum dynamical processes to a fresh consideration. One aspect is the effect of decoherence on

frequency response. A related issue under study is the interconnection between decoherence times, irreversibility and dynamical chaos [50]. Having shown the subtle relation between spectral properties and time dependences, one foresees that our models can provide new insight to this topic. The analysis of the consequences of the spectral complexity of many-body systems is a fully unexplored field ahead. Once again, technology pushes us to the frontiers of the conceptual understanding of Quantum Mechanics and Statistical Physics.

Acknowledgements

We acknowledge P.R. Levstein and F. Toscano for critical discussions. We acknowledge financial support of bi-national programs of Antorchas-Vitae and CONICET-CONICIT as well as local support from SeCyT-UNC. HMP and LEFFT are affiliated with CONICET.

References

- [1] C. Joachim, J.K. Gimzewski, A. Aviram, *Nature* 408 (2000) 541; M.A. Reed, J.M. Tour, *Sci. Am.* 282 (6) (2000) 68.
- [2] C. Dekker, M. Ratner, *Phys. World* 14 (2001) 29.
- [3] H. Frauenfelder, P.G. Wolynes, R.H. Austin, *Rev. Mod. Phys.* 71 (1999) S419.
- [4] P.W. Anderson, *Rev. Mod. Phys.* 50 (1978) 191.
- [5] L. Esaki, *Rev. Mod. Phys.* 46 (1974) 237.
- [6] M. Kastner, *Phys. Today* 46 (1993) 25.
- [7] S. Washburn, R.A. Webb, *Rep. Prog. Phys.* 55 (1993) 1311.
- [8] V.J. Goldman, D.C. Tsui, J.E. Cunningham, *Phys. Rev. B* 36 (1987) 7635.
- [9] B.C. Stipe, M.A. Rezaei, W. Ho, *Phys. Rev. Lett.* 81 (1998) 1263; H. Park et al., *Nature* 407 (2000) 57.
- [10] J.H. Schon, A. Dodabalapur, Z. Bao, Ch. Kloc, O. Schenker, B. Batlogg, *Nature* 410 (2001) 189.
- [11] R. Landauer, *Phys. Lett.* 85A (1981) 91; R. Landauer, *IBM J. Res. Develop.* 1 (1957) 223; R. Landauer, *Philos. Mag.* 21 (1970) 863.
- [12] J.L. D'Amato, H.M. Pastawski, *Phys. Rev. B* 41 (1990) 7411.
- [13] V.L. Nguyen, B.Z. Spivak, B.I. Shklovskii, [*JETP Lett.* 41 (1985) 42], *Pisma Zh. Éksp. Teor. Fiz.* 41 (1985) 35; E. Medina, M. Kardar, *Phys. Rev. B* 46 (1992) 9984.
- [14] M. Büttiker, *Phys. Rev. Lett.* 57 (1986) 1761.
- [15] H.M. Pastawski, *Phys. Rev. B* 46 (1992) 4053.
- [16] M. Büttiker, *IBM J. Res. Dev.* 32 (1988) 63.
- [17] P.O. Löwdin, *J. Chem. Phys.* 19 (1951) 1396, these projection techniques were discussed in the context of a real space Renormalization Group Decimation in; C.E.T. Gonçalves da Silva, B. Koiller, *Solid State Commun.* 40 (1981) 215; J.V. José, *Phys. Rev. Lett.* 49 (1982) 334.
- [18] P. Levstein, H.M. Pastawski, J.L. D'Amato, *J. Phys.: Condens. Matter* 2 (1990) 1781.
- [19] H.M. Pastawski, E. Medina, *Rev Mex. Fis.* 47S1 (2001) 1, also available at cond-mat/0103219.
- [20] L.V. Keldysh, *Zh. Eksp. Teor. Fiz.* 91 (1986) 1815 [*Sov. Phys. JETP* 64 (1986) 1075]; L.P. Kadanoff, G. Baym, *Quantum Statistical Mechanics*, Benjamin, New York, 1962.
- [21] P. Danielewicz, *Ann. Phys. (N. Y.)* 152 (1984) 239.
- [22] D.S. Fisher, P.A. Lee, *Phys. Rev. B* 23 (1981) 6951; F. Sols, *Ann. Phys. (N. Y.)* 214 (1992) 386.
- [23] J.N. Onuchic, P.C.P. de Andrade, D.N. Beratan, *J. Chem. Phys.* 95 (1991) 1131; V. Mujica, M. Kemp, M.A. Ratner, *J. Chem. Phys.* 101 (1994) 6856; M.D. CoutinhoNeto, A.A. daGama, *Chem. Phys.* 203 (1996) 43.
- [24] F. Gagel, K. Maschke, *Phys. Rev. B* 54 (1996) 13889.
- [25] H.M. Pastawski, *Phys. Rev. B* 44 (1991) 6329.

- [26] S. Datta, *J. Phys. Condens. Matter* 2 (1990) 8023;
Electronic Transport in Mesoscopic Systems, Cambridge U. P., Cambridge, 1995, and references therein.
- [27] I. Knittel, F. Gagel, M. Schreiber, *Phys. Rev. B* 60 (1999) 916.
- [28] E.V. Anda, S.S. Makler, H.M. Pastawski, R.G. Barrera, *Braz. J. Phys.* 24 (1994) 330.
- [29] N.S. Wingreen, K.W. Jacobsen, J.W. Wilkins, *Phys. Rev. Lett.* 61 (1988) 1396;
Phys. Rev. B 40 (1989) 11834.
- [30] J.A. Støvneng, E.H. Hauge, P. Lipavský, V. Špička, *Phys. Rev. B* 44 (1991) 13595.
- [31] H. Haug, A.-P. Jauho, *Quantum Kinetics in Transport and Optics of Semiconductors*, Springer, Heidelberg, 1998;
A.P. Jauho, N.S. Wingreen, Y. Meir, *Phys. Rev. B* 50 (1994) 5528.
- [32] R.G. Lake, G. Klimeck, S. Datta, *Phys. Rev. B* 47 (1993) 6427.
- [33] J. Bonča, S.A. Trugman, *Phys. Rev. Lett.* 75 (1995) 2566;
Phys. Rev. Lett. 79 (1997) 4874.
- [34] N. Mingo, K. Makoshi, *Phys. Rev. Lett.* 84 (2000) 3694.
- [35] E.G. Emberly, G. Kirczenow, *Phys. Rev. B* 61 (2000) 5740.
- [36] H. Ness, S.A. Shevlin, A.J. Fisher, *Phys. Rev. B* 63 (2001) 125422.
- [37] J.L. D'Amato, H.M. Pastawski, J.F. Weisz, *Phys. Rev. B* 39 (1989) 3554.
- [38] U. Fano, *Phys. Rev.* 124 (1961) 1866.
- [39] L.E.F. Foa Torres, H.M. Pastawski, S.S. Makler, *Phys. Rev. B* 64 (2001) 193304.
- [40] H.W. Lee, *Phys. Rev. Lett.* 82 (1999) 2358.
- [41] T. Taniguchi, M. Büttiker, *Phys. Rev. B* 60 (1999) 13814.
- [42] K. Haule, J. Bonča, *Phys. Rev. B* 59 (1999) 13087.
- [43] S. Hameau, Y. Guldner, O. Verzelen, R. Ferreira, G. Bastard, J. Zeman, A. Lemaître, J.M. Gérard, *Phys. Rev. Lett.* 83 (1999) 4152;
O. Verzelen, S. Hameau, Y. Guldner, J.M. Gérard, R. Ferreira, G. Bastard, *Jpn. J. Appl. Phys.* 40 (2001) 1.
- [44] M.A. Ratner, *PNAS* 98 (2001) 387.
- [45] E.R. Brown, T.C.L.G. Sollner, C.D. Parker, W.D. Goodhue, C.L. Chen, *Appl. Phys. Lett.* 55 (1989) 1777.
- [46] M. Büttiker, R. Landauer, *Phys. Rev. Lett.* 49 (1982) 1739;
Phys. Scr. 32 (1985) 429;
R. Landauer, Th. Martin, *Rev. Mod. Phys.* 66 (1994) 217.
- [47] A. Nitzan, J. Jortner, J. Wilkie, A.L. Burin, M. Ratner, *J. Phys. Chem. B* 104 (2000) 5661.
- [48] V.N. Prigodin, B.L. Altshuler, K.B. Efetov, S. Iida, *Phys. Rev. Lett.* 72 (1994) 546;
H.M. Pastawski, P.R. Levstein, G. Usaj, *Phys. Rev. Lett.* 75 (1995) 4310;
H.M. Pastawski, G. Usaj, P.R. Levstein, *Chem. Phys. Lett.* 261 (1996) 329.
- [49] E. Medina, H.M. Pastawski, *Phys. Rev. B* 61 (2000) 5850.
- [50] R.A. Jalabert, H.M. Pastawski, *Phys. Rev. Lett.* 86 (2001) 2490.
- [51] F.M. Cucchietti, H.M. Pastawski, R. Jalabert, *Physica A* 283 (2000) 285;
F.M. Cucchietti, H.M. Pastawski, D.A. Wisniacki, *Phys. Rev. E* 65 (2002) 045206 (R).
- [52] C.J. Bolton-Heaton, C.J. Lambert, V.I. Falco, V. Prigodin, A.J. Epstein, *Phys. Rev. B* 60 (1999) 10569.